The EMBO Journal Vol.16 No.14 pp.4467–4476, 1997

MutS mediates heteroduplex loop formation by a translocation mechanism

Dwayne J.Allen[1], Alexander Makhov[3], Michelle Grilley[1,4], John Taylor[1,5], Randy Thresher[3,6], Paul Modrich[1,2] and Jack D.Griffith[3,7]

[1]Department of Biochemistry, Duke University Medical Center, Durham, NC 27710, [2]Howard Hughes Medical Institute, Duke University Medical Center, Durham, NC 27710 and [3]Lineberger Cancer Research Center, University of North Carolina, Chapel Hill, NC 27599-7295, USA

[4]Present address: Department of Biology, Utah State University, Logan, UT 84322, USA
[5]Present address: Department of Molecular Pharmacology, Pfizer Central Research, Sandwich, Ramsgate Road, Kent CT13 9NJ, UK
[6]Present address: Department of Pathology, University of North Carolina, Chapel Hill, NC 27599, USA

[7]Corresponding author

Interaction of *Escherichia coli* MutS and MutL with heteroduplex DNA has been visualized by electron microscopy. In a reaction dependent on ATP hydrolysis, complexes between a MutS dimer and a DNA heteroduplex are converted to protein-stabilized, α-shaped loop structures with the mismatch in most cases located within the DNA loop. Loop formation depends on ATP hydrolysis and loop size increases linearly with time at a rate of 370 base pairs/min in phosphate buffer and about 10 000 base pairs/min in the HEPES buffer used for repair assay. These observations suggest a translocation mechanism in which a MutS dimer bound to a mismatch subsequently leaves this site by ATP-dependent tracking or unidimensional movement that is in most cases bidirectional from the mispair. In view of the bidirectional capability of the methyl-directed pathway, this reaction may play a role in determination of heteroduplex orientation. The rate of MutS-mediated DNA loop growth is enhanced by MutL, and when both proteins are present, both are found at the base of α-loop structures, and both can remain associated with excision intermediates produced in later stages of the reaction.

Keywords: DNA repair/mismatch repair/mutagenesis/mutator

Introduction

Escherichia coli methyl-directed mismatch repair stabilizes the bacterial genome by correcting biosynthetic errors and by ensuring the fidelity of genetic recombination (reviewed by Meselson, 1988; Radman, 1989; Modrich, 1991; Modrich and Lahue, 1996). Repair of biosynthetic errors is strand-specific in that correction is directed to the newly synthesized strand that transiently lacks adenine methylation at d(GATC) sequences. The unmodified strand of hemimethylated heteroduplex DNA is subject to correction, while symmetrically methylated DNA is not (Lu *et al*., 1983; Pukkila *et al*., 1983; Wagner *et al*., 1984). Genetic and biochemical experiments have implicated ten gene products in the methyl-directed reaction [MutS, MutL, MutH, DNA helicase II, single-stranded DNA-binding protein (SSB), exonuclease I, exonuclease VII or RecJ exonuclease, DNA polymerase III holoenzyme and DNA ligase] (Nevers and Spatz, 1975; Lu *et al*., 1983, 1984; Pukkila *et al*., 1983; Lahue *et al*., 1989; Cooper *et al*., 1993) and repair has been reconstituted with purified proteins (Lahue *et al*., 1989; Cooper *et al*., 1993).

Repair is initiated by binding of MutS to a mismatch (Su and Modrich, 1986), followed by binding of MutL (Grilley *et al*., 1989). Assembly of this complex activates a MutH-associated d(GATC) endonuclease, which incises the unmodified strand at a hemimethylated d(GATC) site (Au *et al*., 1992). The DNA strand break produced in this manner serves as the primary signal that directs mismatch correction to the unmethylated strand. This point was established by the demonstration that a pre-existing strand break is not only sufficient to target repair to the incised strand, but also bypasses the requirements for MutH and a d(GATC) site in the reaction (Längle-Rouault *et al*., 1987; Lahue *et al*., 1989).

The excision step of bacterial mismatch repair removes that portion of the unmethylated strand that spans the strand break and the mismatch in a complex reaction dependent on MutS, MutL, the *mutU* gene product DNA helicase II and several exonucleases (Lahue *et al*., 1989; Cooper *et al*., 1993). Excision is strictly exonucleolytic, initiating at the incision and proceeding toward the mismatch to terminate at several discrete sites just beyond the original location of the mispair (Grilley *et al*., 1993). The strand break that directs the reaction can be located on either side of the mismatch. When the strand signal occurs 5′ to the mispair on the unmethylated strand, excision requires a 5′→3′ exonuclease, and either exonuclease VII or RecJ exonuclease will suffice in this respect (Cooper *et al*., 1993). Heteroduplex repair directed by a signal 3′ to the mismatch depends on exonuclease I, a 3′→5′ hydrolytic activity. The three exonucleases implicated in mismatch repair are specific for single-stranded DNA, and excision initiating from either side of the mismatch depends on the cooperative action of DNA helicase II and the appropriate exonuclease (Grilley *et al*., 1993). The excised segment of the unmethylated strand is replaced by new DNA in a reaction that requires DNA polymerase III holoenzyme and SSB, with ligase restoring covalent continuity to the repaired strand (Lahue *et al*., 1989).

The bidirectional excision capability of the methyl-directed system, which has proven to be a characteristic

of strand-specific mismatch repair (Modrich and Lahue, 1996), requires that the repair system evaluate its location on the helix relative to that of the mispair to ensure loading of the proper 5′→3′ or 3′→5′ excision system. The mechanism responsible for determination of heteroduplex orientation operates over substantial helix contour length since a d(GATC) sequence can direct repair of a mismatch at a distance of a kilobase (kb) or more (Lu *et al*., 1983; Längle-Rouault *et al*., 1986; Lahue *et al*., 1987; Bruni *et al*., 1988). Electron microscopy (EM) has been used to examine the interactions of MutS and MutL with heteroduplex DNA to gain further insight into the mechanism of methyl-directed correction and the structural nature of DNA–protein complexes involved in the reaction. We show that MutS mediates formation of α-shaped DNA loops, apparently by a tracking mechanism; that MutL, although not necessary for loop formation, can be a component of loop structures; and that DNA loops may be intermediates in the excision stage of the reaction.

Results

Endonuclease protection by mismatch-bound MutS is reversed upon addition of ATP

In addition to its mismatch binding activity, MutS hydrolyzes ATP to ADP and P_i. The nucleotide hydrolytic center is necessary for biological activity of the protein *in vivo* (Haber and Walker, 1991; Wu and Marinus, 1994), and ATP hydrolysis is required for function of MutS in the initiation of repair *in vitro* (Au *et al*., 1992). We have determined the effect of ATP addition on preformed complexes between MutS and the linear form of a 6.4 kb G–T heteroduplex shown in Figure 1. Binding of MutS protected the heteroduplex against *Nhe*I hydrolysis, with the degree of protection increasing with MutS concentration (Figure 2, upper panel). This effect was mismatch-dependent since MutS afforded no protection of the *Nhe*I site with an otherwise identical homoduplex that contained an A–T base pair in place of the mismatch at position 5632 (not shown). However, different results were obtained when *Nhe*I and ATP were simultaneously added to preformed MutS–mismatch complexes. The presence of ATP rendered the heteroduplex *Nhe*I-sensitive within the 10 s period of exposure to the endonuclease, indicating that ATP either induces a large conformational transition within the MutS–DNA complex, or that the protein leaves the mismatch in the presence of the nucleotide. To determine whether deprotection is dependent upon ATP hydrolysis, similar experiments were performed with ATPγS, an analog which fails to support mismatch-, MutS- and MutL-dependent activation of the latent d(GATC) endonuclease activity of MutH (Au *et al*., 1992). The ATP analog also resulted in some deprotection of the *Nhe*I site (not shown). While we cannot exclude the possibility that some hydrolysis of ATPγS occurred in these reactions, the simplest interpretation of this observation is that ATP binding to mismatch-bound MutS may suffice to drive the conformational transition detected by *Nhe*I endonuclease assay.

Protein-stabilized DNA loops during initiation of mismatch repair

Methyl-directed repair is initiated via mismatch-provoked incision of an unmethylated d(GATC) sequence, a reaction

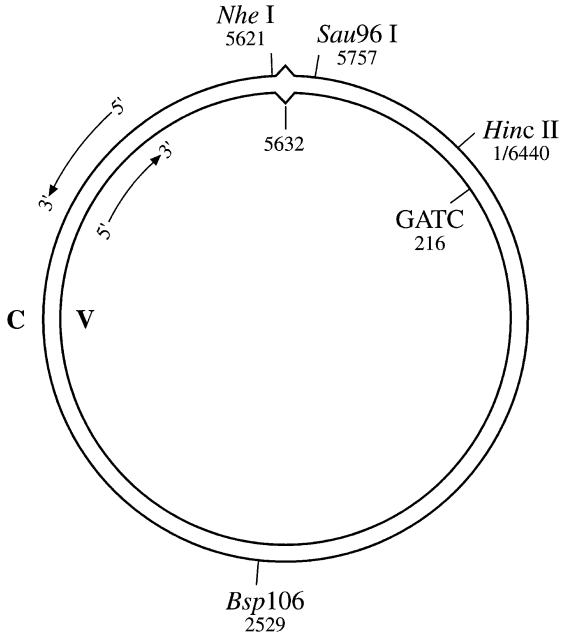

Fig. 1. Heteroduplex DNA. The 6440 bp DNA substrates contained a G–T or C–C mismatch, or a G–C base pair at position 5632 and were linearized with *Bsp*106 at position 2529. Cleavage with this enzyme places the mismatch near the center of the molecule with flanking DNA sequences of 3103 and 3337 bp. The d(GATC) site at position 216, slightly more than 1000 bp from the mismatch (shorter path), was modified as indicated. Substrates used in complete reactions shown in Figure 8 contained a single-strand break in the complementary strand at the *Sau*96I site at position 5757.

that requires MutS, MutL, MutH and ATP and occurs efficiently even when the two DNA sites are separated by a kilobase (Au *et al*., 1992). To clarify the molecular interactions that occur during the early stage of repair, initiation reactions were fixed with glutaraldehyde and visualized by EM. As summarized in Table I, most of the G–T heteroduplexes scored (65–92%) were in the form of protein–DNA complexes, and the majority of these were in the form of α-shaped DNA loops, the structure of which will be considered below. Since yields of complexes with and without a loop were both greatly reduced when homoduplex DNA containing a G–C base pair was substituted for a G–T heteroduplex, complex formation was dependent on presence of a mismatch. Furthermore, the frequency of loop structures depended on the nature of the mismatch. Loop frequency with a C–C heteroduplex was <10% of that observed with G–T substrates, but the incidence of non-looped complexes was similar with the two types of heteroduplex. It is interesting to note in this regard that although MutS binds with weak but significant affinity to the C–C mispair, this mismatch is not subject to methyl-directed correction (Su *et al*., 1988; Lahue *et al*., 1989).

The majority of the heteroduplexes that we have used in these experiments contained a single d(GATC) sequence, which in most cases was hemimethylated with modification on the complementary DNA strand (Figure 1). However, as shown in Table I, formation of looped and non-looped protein–heteroduplex complexes was independent of the state of methylation of the individual DNA strands, and the presence of a d(GATC) sequence within the heteroduplex was not required for loop formation.

Although a small decrease in the frequencies of the two types of complexes was observed with a heteroduplex that contained d(GATT) instead of a d(GATC) site, it is clear that the latter sequence is not necessary for loop formation.

Structure of MutS-stabilized DNA loops

Subsequent experiments demonstrated that MutS, ATP and a mismatch are sufficient for loop formation with the 6.4 kb G–T heteroduplex shown in Figure 1. As shown in Figure 3, a protein complex with apparent dimeric structure was evident at the base of the loop in the α-shaped structures. Although not shown, occasional molecules were observed that contained a second, smaller loop internal to a primary loop.

That portion of the linear G–T heteroduplex contained within MutS-stabilized loops was determined for complexes produced during a 2 min incubation in phosphate buffer or a 15 s incubation in HEPES buffer (Figure 4). The majority of the loops (72% and 80% of those produced in phosphate and HEPES buffers, respectively) were positioned so that they spanned the mismatch, which was located near the center of the linear DNA. In many cases the mismatch was within the loop and some distance from the MutS complex, but molecules with a loop endpoint near the mispair were also relatively common. The remaining 20–28% of the loops observed were located near an end of the linear heteroduplex (Figure 4). The distribution of loop location for molecules that were rapidly frozen in the absence of fixative was similar to that for glutaraldehyde-fixed samples, ruling out a glutaraldehyde crosslinking artifact as a source of the looped structures described here.

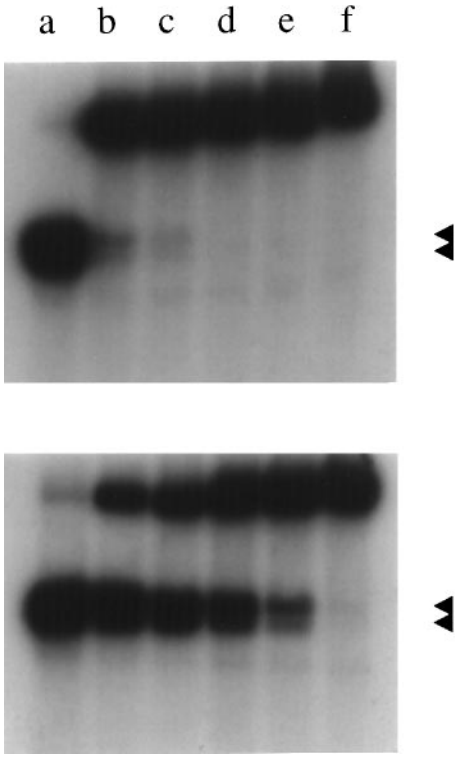

Fig. 2. MutS protection against *Nhe*I cleavage is ATP-dependent. Complexes between MutS and *Bsp*106-linearized, ^{32}P-end-labeled, linear G–T heteroduplex (33 ng, Figure 1) were prepared in 0.01 ml HEPES-buffered reactions as described in Materials and methods, except that KCl and $MgCl_2$ concentrations were 0.01 M and 2 mM, respectively, BSA was present at 50 μg/ml, and ATP was omitted. After equilibration at 37°C, reactions were supplemented with 5 μl of reaction buffer containing 5 units of *Nhe*I (upper panel) or 5 units of *Nhe*I and 150 μM ATP (lower panel). Reactions were terminated after further incubation for 10 s by addition of 8 μl of 0.1 M EDTA, 0.1 M Tris, pH 8.0, 40% (w/v) sucrose and 100 μg/ml bromophenol blue. After electrophoresis through 1% agarose in 0.08 M Tris–phosphate, pH 7.6, 8 mM EDTA, gels were dried and subjected to autoradiography. Samples shown in lanes a–f contained 0, 12, 25, 50, 100 or 200 ng MutS. The 3346 bp and 3094 bp products of *Nhe*I hydrolysis, which cleaves the heteroduplex 11 bp from the mismatch (position 5621, Figure 1), are indicated by arrowheads.

DNA loop growth is ATP-dependent and linear with time

MutS-mediated formation of heteroduplex loops was not observed in the absence of ATP and, as shown in Figure 5, the size of DNA loops produced with a G–T substrate was dependent on ATP concentration. The nucleotide dependence of loop formation displayed apparent saturability, with a K_m of 0.3 mM, a value identical to that determined for mismatch- and MutHLS-dependent cleavage at a d(GATC) sequence, albeit under different buffer conditions (Au *et al*., 1992).

The rapid rate of loop growth in HEPES buffer precluded kinetic study of the reaction under the conditions used for *in vitro* mismatch repair assay (Lahue *et al*., 1989), but it was possible to follow the kinetics of loop growth in phosphate-buffered reactions (Materials and methods). Under these conditions, average loop size with a G–T heteroduplex increased in a near-linear fashion at a rate of 340–370 base pairs (bp) per min (Figure 6).

Several lines of evidence indicate that ATP hydrolysis is necessary for this process. Loop yield in HEPES buffer was reduced by 90% when 2 mM ATP was replaced by 2 mM ATPγS, and by 80% when both nucleotides were present at 2 mM (not shown). Furthermore, addition of a

Table I. DNA substrate requirements for loop formation

Mismatch and methylation (C/V)	Protein free	Protein bound no loop	Protein bound with loop (%)	Molecules counted
G^+/T^-	8	29	63	175
G^-/T^+	15	31	54	151
G^0/T^0	35	21	44	127
C^+/C^-	64	32	4	240
G^+/C^-	92	5	3	166

HEPES-buffered reactions (Materials and methods) contained 10 μg/ml *Bsp*106-linearized heteroduplex or homoduplex DNA (Figure 1), 14 μg/ml MutS, 4 μg/ml MutL and 0.42 μg/ml MutH. After incubation at 37°C for 15 min, samples were glutaraldehyde-fixed and prepared for EM. The 'Mismatch and methylation' column indicates the base pair at position 5632 and in superscript notation, the state of complementary (C) and viral (V) strand modification at the single d(GATC) sequence in the substrate. A superscript '0' indicates that the heteroduplex contained d(GATT) instead of a d(GATC) sequence at coordinate 216.

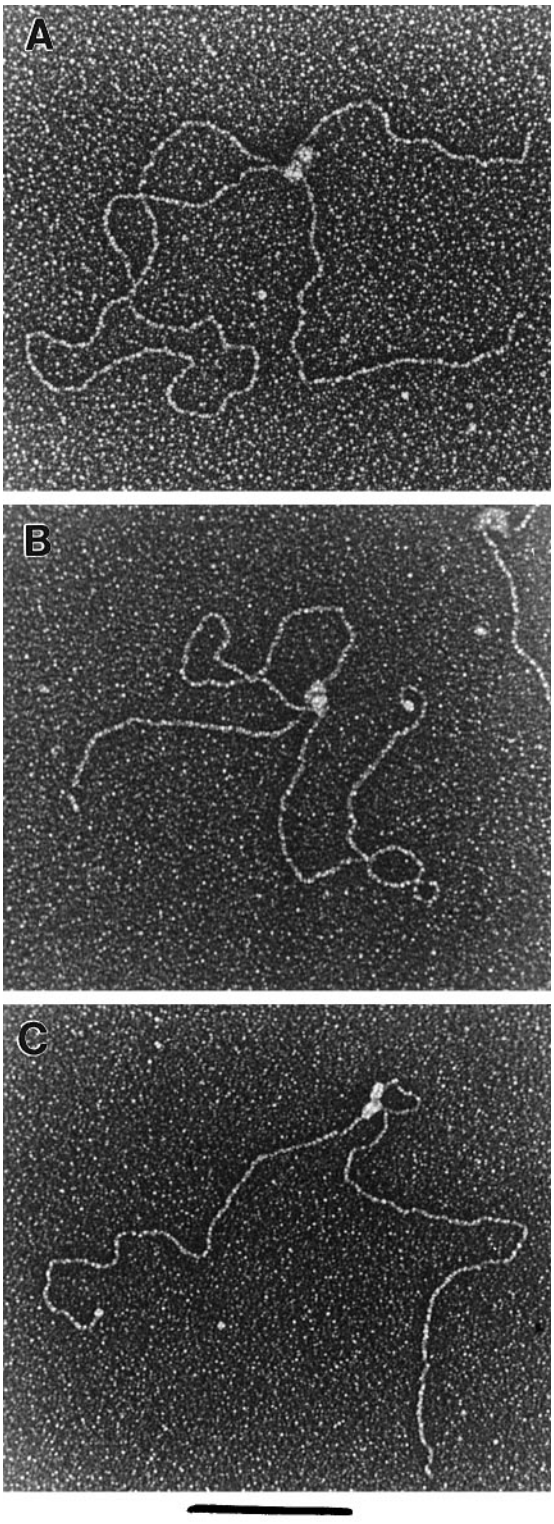

Fig. 3. MutS-mediated DNA loop formation with heteroduplex DNA. Samples were glutaraldehyde-fixed and prepared for electron microscopy as described in Materials and methods, including adsorption to thin carbon foils and rotary shadow casting with tungsten. Shown in reverse contrast. The bar corresponds to 1.6, 1.3 and 1.0 kb for panels A, B and C, respectively. (**A**) A phosphate-buffered reaction contained 7.5 μg/ml linear G–T heteroduplex, 10 μg/ml MutS and 2 mM ATP. Incubation was at 37°C for 8 min. (**B**) and (**C**) HEPES-buffered reactions contained 15 μg/ml linear G–T heteroduplex, 12.5 μg/ml MutS and 2 mM ATP. Incubation was for 15 s.

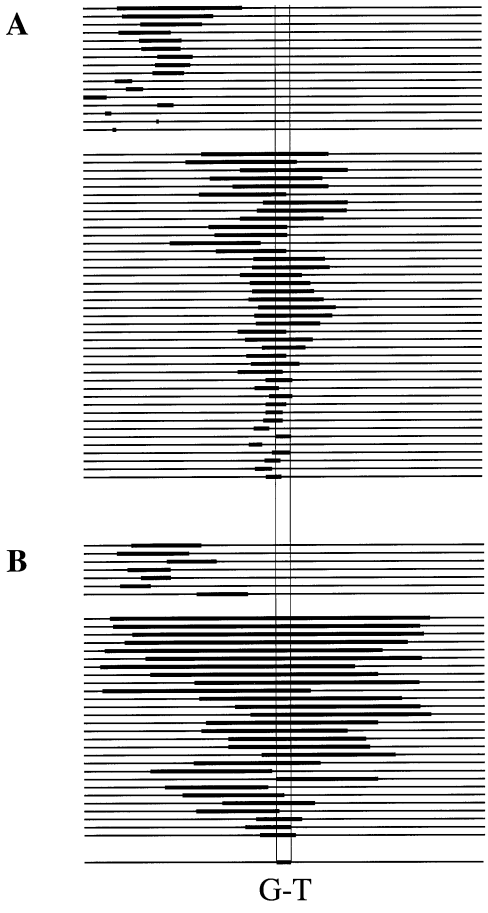

Fig. 4. Location of MutS-stabilized DNA loops. Samples were prepared for electron microscopy and loop-size analysis performed as described in Materials and methods. The G–T heteroduplex was linearized with *Bsp*106, which places the mismatch near the center of the molecule, 3104 bp from one end and 3336 bp from the other. Since loop placement was determined relative to heteroduplex ends without regard to orientation, there is a 232 bp uncertainty with respect to location of the mismatch. This is indicated by the vertical lines. (**A**) Phosphate-buffered reactions contained 7.5 μg/ml linear G–T heteroduplex, 10 μg/ml MutS and 2 mM ATP. Incubation was at 37°C for 2 min followed by glutaraldehyde fixation. (**B**) HEPES-buffered reactions contained 15 μg/ml linear G–T heteroduplex, 12.5 μg/ml MutS and 2 mM ATP. After incubation at 37°C for 15 s, samples were deposited directly onto grids and frozen in liquid ethane.

50-fold excess of AMP-PNP to loops growing in the presence of ATP in phosphate buffer blocked further increase in loop size, but loops formed prior to addition of the analogue were stable (Figure 6, upper panel). Based on these observations, we conclude that hydrolysis of ATP by MutS is necessary for loop growth, but not for maintenance of loops once formed.

As noted above, the rate of loop growth in the HEPES buffer used for mismatch repair assay (Lahue *et al*., 1989) is too fast to permit study of kinetics of the reaction. We think it likely that the rate reduction in phosphate buffer is due to end-product inhibition of the MutS-associated ATPase, which hydrolyzes ATP to ADP and P_i (Haber and Walker, 1991; Au *et al*., 1992). Although we have been unable to study kinetics in HEPES buffer, the average loop size of 2500 bp (range 430–5500 bp) observed after 15 s (Figure 4B) indicates that the rate of loop growth is

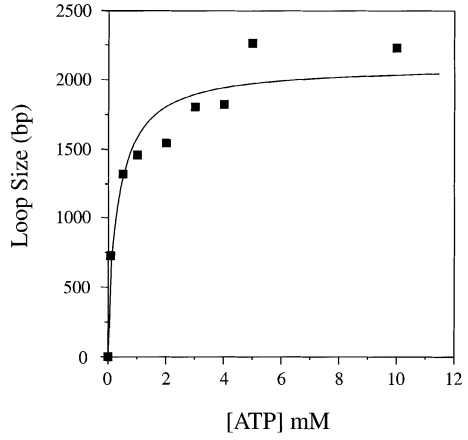

Fig. 5. ATP-dependence of loop formation. Phosphate-buffered reactions with a linear G–T heteroduplex were performed as described in the legend to Figure 3 except ATP concentration was varied as indicated. Incubation was for 4 min, and loop-size analysis performed as described in Materials and methods. The curve shown was determined by non-linear least-squares fit to a hyperbola (Marquardt, 1963) and is characterized by an apparent K_m of 0.3 mM.

~10 000 bp/min, more than 30-fold that observed in phosphate-buffered reactions.

The oligomeric state of active MutS

Sedimentation of purified MutS has suggested that the protein exists in solution as dimers and tetramers of a 95 kDa polypeptide (Su and Modrich, 1986). The protein complex at the base of heteroduplex loops (Figure 3) exhibits dimeric structure, but could also represent a higher oligomeric state. (Note that under conditions of MutS excess—much greater than that described here—very large heteroduplex-bound complexes were observed, suggesting that MutS may aggregate at high concentrations.) To estimate the mass of MutS bound to the 6.4 kb G–T heteroduplex in the presence of ATP, β-amylase was added as an internal molecular weight standard prior to EM visualization. Micrographs were taken in which at least five β-amylase molecules were present in a MutS–heteroduplex field, and the mean projected areas of the β-amylase and MutS complexes were determined (Materials and methods). Based on the 200 kDa mass of β-amylase, area ratios provided an estimate for the mass of the MutS complex corrected for local variations in metal coating during EM preparation (Griffith *et al*., 1995). Of 30 MutS–DNA complexes analyzed, 24 were between 160 and 280 kDa, with an average mass of 217 kDa (Figure 7, upper panel). Since this value includes the DNA mass within an individual complex and inasmuch as the monomeric subunit molecular weight of MutS is 95 kDa, the protein apparently binds to the 6.4 kb G–T heteroduplex as a dimer.

An independent assessment of the mass of active MutS was obtained by use of Surface Plasmon Resonance spectroscopy to monitor binding of the protein to 31 bp G–T heteroduplex and A–T homoduplex DNAs (Materials and methods). A mismatch-specific signal due to MutS binding was observed (Figure 7, lower panel), and the ratio of the mass of bound MutS to the mass of the heteroduplex was determined from plateau values at the higher MutS concentrations where equilibrium was effectively achieved. This method yielded a value of 10.3 for the protein–DNA mass ratio in the specific complex, corresponding to a MutS mass of 210 kDa, or 2.2 monomer equivalents per 31 bp heteroduplex. In contrast to the EM mass estimate, this determination was performed in the absence of ATP and thus scores binding of the protein to the G–T mismatch in the small duplex.

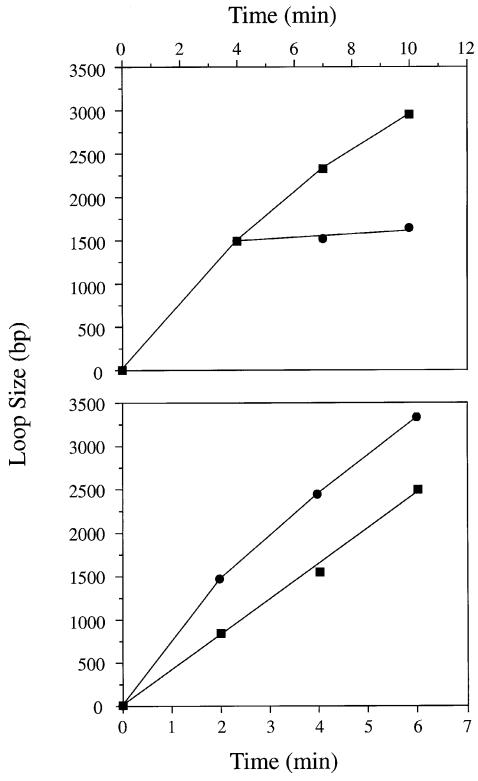

Fig. 6. Kinetics of loop formation. Phosphate-buffered reactions with a linear G–T heteroduplex were performed as described in the legend to Figure 3 and reactions terminated by glutaraldehyde fixation at times indicated. Loop-size analysis was performed as described in Materials and methods. Upper panel: parallel reactions contained 1 mM ATP and 10 μg/ml MutS. At 4 min, buffer (■) or AMP-PNP (●, 50 mM) was added and incubation continued. Lower panel: reactions contained 2 mM ATP and 10 μg/ml MutS (■) or 10 μg/ml MutS and 12 μg/ml MutL (●).

MutL stimulates heteroduplex loop growth and is present in looped complexes

Although MutS is sufficient for mismatch recognition and heteroduplex loop formation, MutL has been shown to bind to the MutS–mismatch complex in a reaction that requires ATP, but apparently not ATP hydrolysis (Grilley *et al*., 1989). MutL is also required for MutS- and mismatch-dependent events that occur at secondary sites on the helix, including MutH activation (Au *et al*., 1992) and excision initiating at a strand break in a pre-incised heteroduplex (Lahue *et al*., 1989). The effect of MutL on MutS-mediated heteroduplex loop formation was therefore examined. As shown in Figure 6 (lower panel), MutL enhanced the rate of loop growth in phosphate buffer from 380 bp/min to 630 bp/min. MutL was also found consistently to increase the yield of looped molecules in the HEPES buffer conditions used for repair assay (not shown).

To test the possibility that MutL might be present in

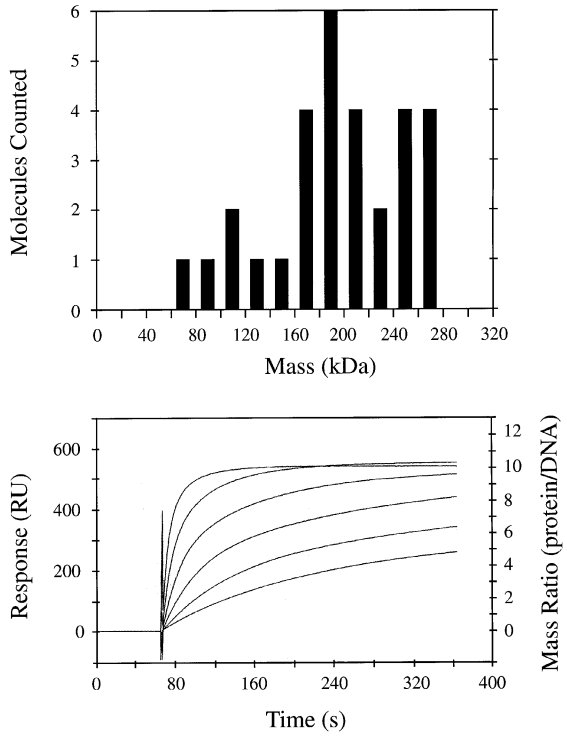

Fig. 7. Size determination of bound MutS. Upper panel: MutS–GT heteroduplex complexes were prepared in phosphate buffer containing 2 mM ATP and glutaraldehyde-fixed as described in the legend to Figure 3 (4 min incubation). The mass of heteroduplex-bound MutS was estimated by EM relative to glutaraldehyde fixed β-amylase added to the samples just before grid adsorption (Materials and methods). Lower panel: binding of MutS to a 31 bp G–T heteroduplex was scored by surface plasmon resonance as described in Materials and methods. The streptavidin sensor chip was derivatized with 56 resonance units (RU) of biotin end-labeled heteroduplex and probed with MutS at concentrations of 12, 25, 50, 100, 200 and 400 nM. The mass of bound MutS per mass unit of heteroduplex was estimated from plateau values of the 200 nM and 400 nM titration curves according to the relation $Mass_{ratio} = (RU_{max,\ G–T}–RU_{max,\ A–T})/(0.79\times56)$, where $RU_{max,\ G–T}$ and $RU_{max,\ A–T}$ correspond to plateau values achieved with chips derivatized with the G–T heteroduplex and an otherwise identical A–T homoduplex. RU_{max} values obtained with the homoduplex control were 14% and 15% of that obtained with the G–T heteroduplex (not shown). The factor 0.79 corrects for the fact that the refractive index increment for a typical protein is 79% of that obtained with an equivalent mass of DNA (Fisher *et al.*, 1994).

looped molecules, MutS–heteroduplex structures prepared in the presence of the former protein were probed with polyclonal antibodies, and the immune complexes tagged with gold-labeled protein A and visualized by EM. As illustrated in Figure 8, protein complexes at the base of heteroduplex loops were tagged with antibody to MutL. Although not shown in Figure 8, similar results were obtained with anti-MutS, indicating that when both proteins are present, both can be located within the protein complex at the base of the DNA loops.

MutS and MutL can remain associated with heteroduplex excision intermediates

It has been previously shown that a pre-incised heteroduplex is subject to mismatch repair in a MutH-independent reaction (Längle-Rouault *et al.*, 1987; Lahue *et al.*, 1989). Mismatch-provoked excision on such molecules requires MutS, MutL, DNA helicase II and an appropriate exonuclease, and may also depend on SSB (Cooper *et al.*, 1993; Grilley *et al.*, 1993). When the incision is 5′ to the mismatch, either exonuclease VII or Rec J exonuclease will suffice for the exonuclease requirement. Tagging of immune complexes with gold-labeled protein A was used to test the possibility that MutS and MutL may remain associated with excision intermediates in the repair reaction. The substrate used for these experiments was a *Bsp*106 linearized G–T heteroduplex containing an incision in the complementary DNA strand at the *Sau*96I site 125 bp 5′ to the mismatch (Figure 1). Examination of excision products produced in the presence of MutS, MutL, helicase II, SSB and exonuclease VII revealed SSB-coated, single-stranded gaps, which in some cases were in looped structures. The presence of MutS and MutL near the junction of single-stranded and duplex DNA was demonstrated using appropriate antibodies and gold-labeled protein A (Figure 8, panels C and D).

Discussion

MutS mediates the efficient conversion of heteroduplex DNA to looped structures in a reaction dependent on a mismatch and ATP hydrolysis. The finding that loop size increases with time in a near-linear fashion is difficult to reconcile with a DNA bending model for loop formation (Schleif, 1992), but is consistent with a mechanism in which the MutS dimer migrates along the helix by directional tracking or unidimensional movement. A mechanism of this type which can account for the observations described here is shown in Figure 9. The MutS dimer in this model has three DNA binding sites: a mismatch binding site, perhaps located at the subunit–subunit interface, and a secondary DNA binding site in each subunit that functions in translocation. ATP reduces affinity of the MutS dimer for the mismatch and activates the binding sites used for translocation. The latter sites draw flanking DNA toward the protein complex in a bidirectional manner, extruding the original DNA binding site into a loop. This mechanism accounts for restriction endonuclease exposure results, for the linear kinetics of loop growth and for the presence of the mismatch within the loop in the majority of the structures observed. The subset of loops with an endpoint near the mispair can be accommodated within this scheme if the DNA translocation site in one subunit occasionally fails to activate.

While the majority of MutS–heteroduplex loops encompass the mispair, about one-quarter of the loops observed comprised sequences external to the mismatch (Figure 4). Since these structures were not observed with homoduplex controls, a mismatch is evidently necessary for their production. It is possible that these molecules reflect presence of a spontaneous mutation in a subset of one of the phage DNA populations that was used for heteroduplex construction, and hence that some heteroduplexes contain a second mismatch. An alternate origin for these molecules attributes their formation to internal rearrangement of large loops that have grown from a single mispair (Figure 9, bottom).

The nature of MutS-induced loops and the mechanism shown in Figure 9 are similar to those recently described for the HSV-1 UL9 helicase acting at the HSV-1 oriS element (Makhov *et al.*, 1996). Two UL9 dimers were

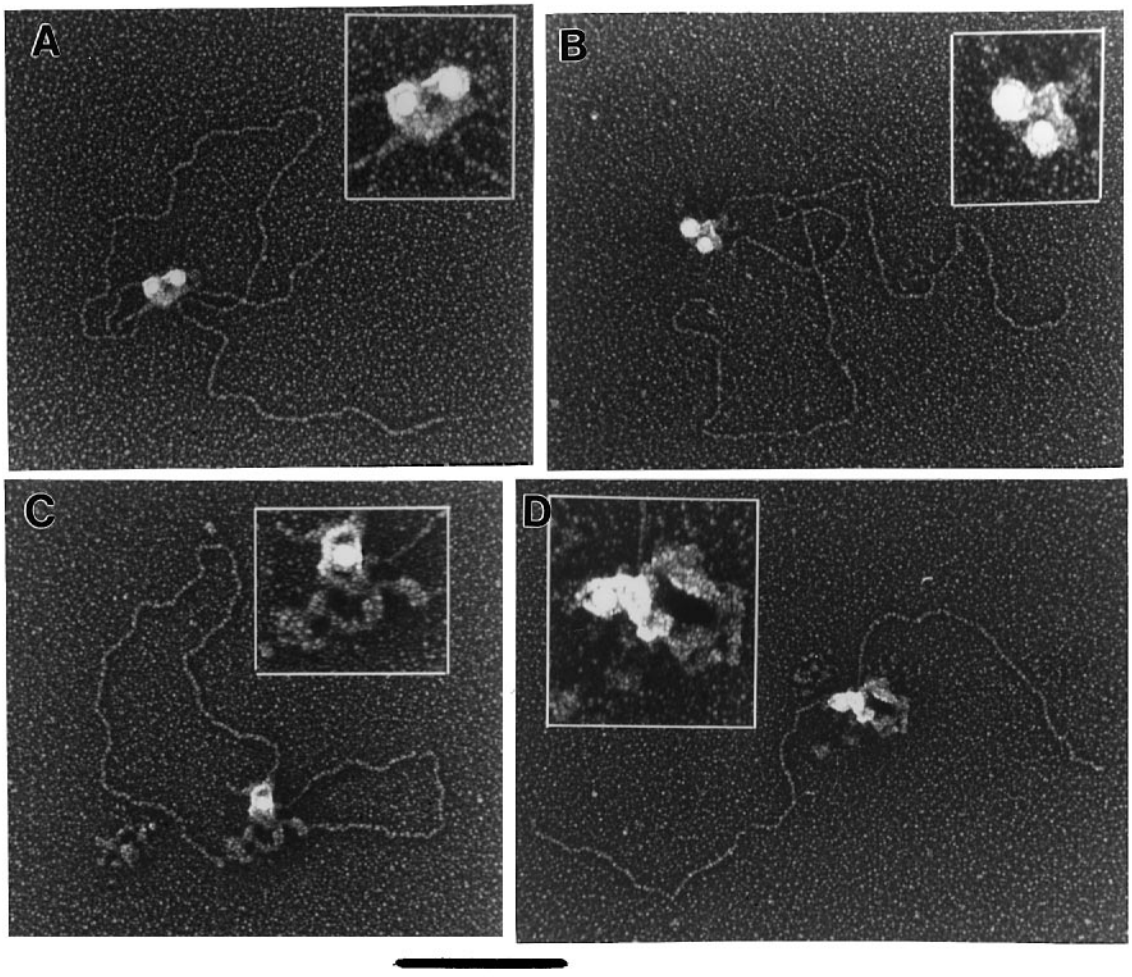

Fig. 8. Localization of MutS and MutL in repair intermediates. Phosphate-buffered reactions contained 7.5 μg/ml linear G–T heteroduplex, 2 mM ATP and repair proteins as indicated, with incubation at 37°C. After glutaraldehyde fixation, samples were supplemented with MutS or MutL antibodies and gold-labeled protein A (Materials and methods). Gold-labeled protein–DNA complexes were not observed in control samples without added antibody. Preparation for EM was as in Figure 3. The bar equals 1 kb. (**A**) Reactions contained MutS only (10 μg/ml) and incubation was for 4 min. Protein–DNA complexes were probed with anti-MutS. (**B**) Reactions contained 10 μg/ml MutS and 12 μg/ml MutL. Protein–DNA complexes were probed with anti-MutL. (**C** and **D**) The linear heteroduplex contained a site-specific incision in the complementary strand at the *Sau*96I site, 126 bp 5′ to the mismatch. Reactions contained 10 μg/ml MutS, 12 μg/ml MutL, 10 μg/ml DNA helicase II, 20 μg/ml SSB and 5 μg/ml exonuclease VII. After a 15 min incubation and glutaraldehyde fixation, samples were probed with anti-MutS (C) or anti-MutL (D).

observed by EM to bind to a bipartite DNA binding site and in doing so kinked the DNA to facilitate the interaction of the UL9 monomers, presumably through their N-termini. In the presence of ATP, each UL9 dimer will translocate DNA, unwinding the DNA in the process. In this case, tethered to each other by their N-termini, the result observed by EM was the formation of ATP-dependent loops of partially unwound DNA. Measurement of the position of the loop relative to the site of initiation (oriS) showed a pattern strikingly similar to the results described here with MutS. In particular, while most of the loops were arranged with equal amounts of DNA on either side of the point of initiation, others had grown only leftwards or only rightwards from oriS. The latter class of molecules was attributed to situations in which one of the two UL9 dimers had bound to oriS and associated with the other UL9 dimer, but was unable to hydrolyze ATP.

Should MutS movement on the helix occur along a groove, the extruded loop might be expected to be superhelical. However, EM visualization provided no indication of superhelicity in these structures. Furthermore, previous work has shown that tertiary structure of covalently closed, superhelical heteroduplexes is not altered when the DNA is incubated with all the components of the methyl-directed system except MutH (Au *et al*., 1992), seemingly excluding topoisomerase involvement in the reaction. These observations suggest that MutS movement is not restricted to a groove or that the dimer can act as a swivel to relieve superhelical tension that would result from migration along a groove.

While the requirement for ATP hydrolysis in loop growth is clear, the manner in which nucleotide binding and hydrolysis is coupled to departure from the mismatch and movement along the helix is not. Since addition of ATPγS to a MutS–mismatch complex renders an adjacent region of helix sensitive to restriction endonuclease attack, ATP binding may drive a MutS conformational transition, perhaps one step in a cycle of conformational changes required for translocation along the helix. However, we do not regard this point as established because some

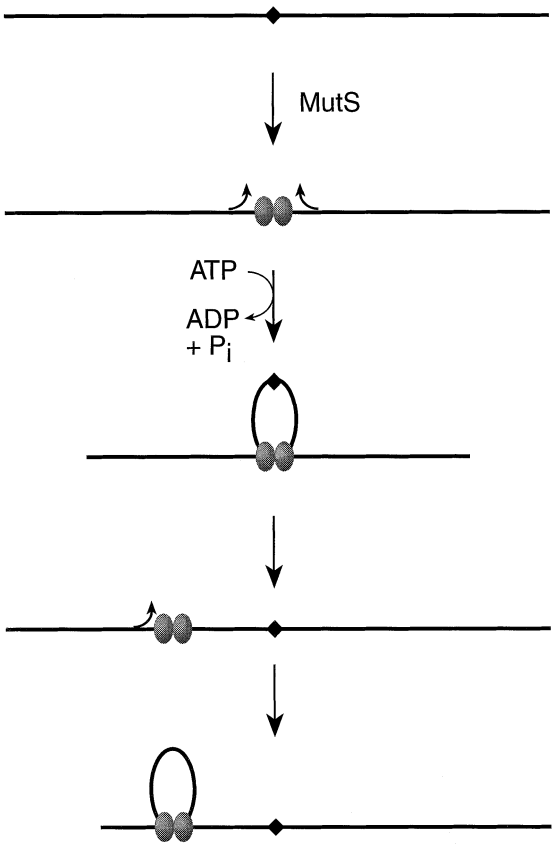

Fig. 9. Model for movement of MutS dimer along a heteroduplex. Details of the mechanism are discussed in the text.

hydrolysis of the ATP analog may have occurred in our experiments. The stoichiometry of ATP hydrolysis relative to translocation distance along the helix also remains to be clarified. The MutS dimer hydrolyzes ATP at rates in the range of 1 to 10 min^{-1} (moles of ATP per mole of MutS dimer per minute), depending on conditions (Haber and Walker, 1991; Au *et al*., 1992; W.Bedale and P.Modrich, unpublished results), but the rate of nucleotide hydrolysis has not been determined for a MutS dimer that has left a mismatch to move along a heteroduplex.

Although no simple activities have been linked to MutL, the protein binds to the MutS–mismatch complex in the presence of ATP or ATPγS (Grilley *et al*., 1989) and is required for coupling mismatch recognition by MutS to MutH activation (Au *et al*., 1992) and to excision (Lahue *et al*., 1989; Grilley *et al*., 1993). We have found that MutL stimulates the rate of MutS-mediated loop growth and is physically located at the base of the loop in the vicinity of bound MutS. These observations suggest that MutS–heteroduplex–MutL loop complexes are important intermediates in mismatch repair. Further support for this view was provided by visualization of excision intermediates produced with an incised heteroduplex in the presence of MutS, MutL, helicase II, SSB and exonuclease VII. Inasmuch as SSB-coated gaps in these intermediates were in some cases arranged in a loop structure with MutL and MutS at the base, it is possible that excision may occur within a looped intermediate.

Methyl-directed repair involves interaction of two DNA sites that can be separated by distances on the order of a kilobase. The finding that MutS mediates heteroduplex loop formation not only provides a simple mechanism for interaction of the two sites, but may also resolve the puzzling question of how the system achieves its bidirectional excision capability. [We do not mean to imply that MutS recognizes a d(GATC) sequence but rather that the MutS–heteroduplex–MutL complex acts as a substrate for addition of other repair activities such as MutH, which is known to be the activity that incises the helix at unmethylated d(GATC) sequences (Lahue *et al*., 1989; Au *et al*., 1992).] The strand break that directs repair may reside either 3′ or 5′ to the mismatch, and excision initiates at this site (Cooper *et al*., 1993; Grilley *et al*., 1993). This requires that the repair system assess placement of the strand break relative to the mismatch, an effect that can be achieved only by transmission of a signal between the two sites along the contour of the helix. The mechanism for loop formation illustrated in Figure 9 would suffice in this respect.

The involvement of heteroduplex loops in mismatch repair requires that these structures be generated at a rate sufficient to be kinetically significant intermediates in the reaction. As noted above, loop growth in the buffer used for mismatch repair assay is extremely fast, ~10 000 bp/min. Furthermore, parallel comparison of loop frequency and mismatch-provoked d(GATC) incision of a hemimethylated G–T heteroduplex has indicated that loop formation is sufficiently fast to account for interaction of the two DNA sites during the initiation stage of repair. Thus, the frequency of loops in 1 min reactions containing MutS, MutL and MutH was comparable with the 40–60% value determined after 15 minutes (Table I; M.Grilley, P.Modrich and J.D.Griffith, unpublished results). By contrast, only 15% of the molecules were subject to d(GATC) incision during the first minute, with this value increasing to 82% by 15 minutes. These observations prove that loop formation is fast relative to d(GATC) cleavage by activated MutH and are consistent with a role for loop structures as intermediates in the initiation step of the methyl-directed repair.

Materials and methods

Proteins and DNA substrates

MutS, MutL, MutH, DNA helicase II and exonuclease VII were isolated as described (Su and Modrich, 1986; Welsh *et al*., 1987; Grilley *et al*., 1989; Cooper *et al*., 1993; Runyon *et al*., 1993). Proteins were diluted into 0.05 M KPO_4, pH 7.4, 0.05 M KCl, 0.1 mM EDTA, 1 mM 2-mercaptoethanol. Other proteins were from commercial sources.

Phage f1MR DNAs used for heteroduplex construction have been described (Lahue *et al*., 1987; Su *et al*., 1988). The 6440 base pair DNA substrates contained a G–T mismatch (prepared from f1MR1 and f1MR3), a C–C mispair (prepared from f1MR8 and f1MR9), or a G–C Watson–Crick base pair (prepared from f1MR3) at coordinate 5632 and a single d(GATC) sequence at coordinate 216 (Figure 1). Unless indicated otherwise, the d(GATC) site was hemimethylated with modification on the complementary DNA strand. A G–T heteroduplex, identical to that shown in Figure 1 except for the presence of a d(GATT) sequence instead of d(GATC) at position 216, was prepared as described previously (Lahue *et al*., 1987). With one exception, heteroduplex DNAs were prepared in covalently closed circular form (Su *et al*., 1988) and subsequently linearized by cleavage at the unique *Bsp*106 site at position 2529, followed by phenol and ether extraction, ethanol precipitation and resuspension in 0.01 M Tris–HCl, pH 7.6, 1 mM EDTA. When indicated, linearized heteroduplex was ^{32}P-end-labeled by incubation with Klenow DNA polymerase I and [α-^{32}P]dCTP in the presence of the other three unlabeled nucleotides. A circular G–T heteroduplex containing a site-

specific incision in the complementary strand at the *Sau*96I site (Figure 1) was prepared from f1MR1 and f1MR3 as described previously (Fang and Modrich, 1993) and linearized with *Bsp*106 as described above.

Preparation of protein–DNA complexes and electron microscopy

Two buffer conditions were used to prepare protein–DNA complexes. HEPES-buffered reactions (0.02–0.05 ml), similar to those used previously to study mismatch repair in a reconstituted system (Lahue *et al*., 1989), contained 0.05 M HEPES–KOH, pH 8.0, 0.02 M KCl, 6 mM $MgCl_2$, 1 mM dithiothreitol, DNA, repair proteins and ATP as indicated. Incubation was at 37°C. Phosphate-buffered reactions were performed in a similar manner except that 0.02 M KPO_4, pH 7.4, was substituted for HEPES–KOH. In some cases reactions were supplemented with (or ATP was replaced by) adenosine-5′-*O*-(3-thiotriphosphate) (ATPγS) or 5′-adenylylimidodiphosphate (AMP-PNP, Calbiochem). All reactions were performed at 37°C.

For preparation of crosslinked protein–DNA complexes, reactions were terminated by addition of glutaraldehyde to 0.6%. After incubation for 10 min at room temperature, DNA and protein–DNA complexes were separated from unbound proteins by filtration through 2 ml columns of Bio-Gel A-5m (Bio Rad Inc.) washed with 0.01 M Tris–HCl, pH 7.6, 0.1 mM EDTA. Filtered samples were mixed with an equal volume of a buffer containing 4 mM spermidine, adsorbed to glow-charged thin carbon foils, dehydrated through a water–ethanol series and rotary shadowcast with tungsten as described (Griffith and Christiansen, 1978).

Reactions for cryo-electron microscopy without glutaraldehyde fixation were carried out in HEPES buffer for 15 s at 37°C, and samples were adsorbed directly onto thin carbon foils. After 5 s, carbon films were washed in double-distilled, deionized water for 3 min, had their excess water blotted off, and were rapidly frozen in liquid ethane chilled with liquid nitrogen. Samples were freeze-dried and rotary shadowcast in a cryopumped Wiltek-modified Balzers 300 freeze-etch machine at 1×10^{-7} torr (Griffith *et al*., 1995). Samples were visualized in Philips EM400 TLG and CM12 instruments. Micrographs for publication were scanned from negatives using a Nikon multiformat film scanner and the contrast optimized and panels arranged using Adobe Photoshop.

Electron microscopy (EM) mass measurement of the MutS particles bound to DNA followed Griffith *et al*. (1995). In brief, MutS–DNA complexes were fixed with 0.6% glutaraldehyde for 5 min at room temperature and isolated by gel filtration. Just before adsorption to the EM supports, β-amylase (Sigma), which had been fixed in the same manner, was added to a concentration of 1 μg/ml and the mixture processed for EM. Micrographs were taken of fields in which a MutS complex was present on the DNA at the site of the mismatch and there were at least five β-amylase particles nearby. Using a COHU CCD camera attached to a Macintosh computer and the NIH IMAGE software, the mean projected area of the β-amylase particles was determined and compared with the projected area of the MutS particle. Calculation of the MutS particle mass based on the 200 kDa mass of β-amylase was done as previously described (Griffith *et al*., 1995). Morphometry measurements were carried out using a Summagraphics digitizer coupled to a Macintosh computer programmed with software developed by J.D.G.

Immunogold labeling of repair intermediates was performed on glutaraldehyde-fixed samples that were prepared in phosphate buffer as described above. Rabbit anti-MutS or rabbit anti-MutL antibody was added to 8.5 μg/ml followed by addition of gold-labeled protein A (G10 Auroprobe EM, 10 nm gold particle, Amersham) to 0.2 μg/ml. Mixtures were incubated at room temperature for 30 min, filtered through BioGel A5m, applied to thin carbon foils and processed for EM as described above. MutS and MutL antibodies used responded to only the appropriate species in Western blots of *Escherichia coli* cell extracts.

Surface plasmon resonance measurements

Surface plasmon resonance measurements were performed on a BIAcore 2000 at 25°C. A streptavidin sensor chip (SA chip, Pharmacia) was derivatized with a 31 bp biotinylated G–T heteroduplex prepared from 5′-biotin-GCCGAATTTCTAGAATCGAGAGCTTGCTAGC and 5′-GCTAGCAAGCTTTCGATTCTAGAAATTCGGC by heating to 80°C and cooling to room temperature over a 2 h period. An otherwise identical A–T homoduplex was prepared by hybridizing 5′-biotin-GCCGAATTTCTAGAATCGAAAGCTTGCTAGC to the latter oligonucleotide. Binding of MutS to the heteroduplex or homoduplex modified SA chips was performed at a flow rate of 20 μl/min in 0.01 M HEPES–KOH, pH 7.4, 0.15 M NaCl, 3.4 mM EDTA, 8.4 mM $MgCl_2$, 0.005% Surfactant P20. The heteroduplex-modified SA chip was regenerated following MutS binding by a 20 μl injection of 0.5% sodium dodecyl sulfate.

Acknowledgements

This work was supported by grants GM23719 (to P.M.) and GM31819 (to J.D.G.) from the National Institute of General Medical Sciences.

References

Au,K.G., Welsh,K. and Modrich,P. (1992) Initiation of methyl-directed mismatch repair. *J. Biol. Chem.*, **267**, 12142–12148.

Bruni,R., Martin,D. and Jiricny,J. (1988) d(GATC) sequences influence *Escherichia coli* mismatch repair in a distance-dependent manner from positions both upstream and downstream of the mismatch. *Nucleic Acids Res*, **16**, 4875–4890.

Cooper,D.L., Lahue,R.S. and Modrich,P. (1993) Methyl-directed mismatch repair is bidirectional. *J. Biol. Chem.*, **268**, 11823–11829.

Fang,W.-H. and Modrich,P. (1993) Human strand-specific mismatch repair occurs by a bidirectional mechanism similar to that of the bacterial reaction. *J. Biol. Chem.*, **268**, 11838–11844.

Fisher,R.J., Fivash,M., Casas-Finet,J., Bladen,S. and McNitt,K.L. (1994) Real-time BIAcore measurements of *Escherichia coli* single-stranded DNA binding (SSB) protein to polydeoxythymidylic acid reveal single-state kinetics with steric cooperativity. *Methods*: *Comp. Methods Enzymol.*, **6**, 121–133.

Griffith,J.D. and Christiansen,G. (1978) Electron microscope visualization of chromatin and other DNA–protein complexes. *Annu. Rev. Biophys. Bioeng.*, **7**, 19–35.

Griffith,J.D., Makhov,A., Zawel,L. and Reinberg,D. (1995) Visualization of TBP oligomers binding and bending the HIV-1 and adeno promoters. *J. Mol. Biol.*, **246**, 576–584.

Grilley,M., Welsh,K.M., Su,S.-S. and Modrich,P. (1989) Isolation and characterization of the *Escherichia coli mutL* gene product. *J. Biol. Chem.*, **264**, 1000–1004.

Grilley,M., Griffith,J. and Modrich,P. (1993) Bidirectional excision in methyl-directed mismatch repair. *J. Biol. Chem.*, **268**, 11830–11837.

Haber,L.T. and Walker,G.C. (1991) Altering the conserved nucleotide binding motif in the *Salmonella typhimurium* MutS mismatch repair protein affects both its ATPase and mismatch binding activities. *EMBO J.*, **10**, 2707–2715.

Lahue,R.S., Su,S.-S. and Modrich,P. (1987) Requirement for d(GATC) sequences in *Escherichia coli mutHLS* mismatch correction. *Proc. Natl Acad. Sci. USA*, **84**, 1482–1486.

Lahue,R.S., Au,K.G. and Modrich,P. (1989) DNA mismatch correction in a defined system. *Science*, **245**, 160–164.

Längle-Rouault,F., Maenhaut-Michel,G. and Radman,M. (1986) GATC sequence and mismatch repair in *Escherichia coli*. *EMBO J.*, **5**, 2009–2013.

Längle-Rouault,F., Maenhaut,M.G. and Radman,M. (1987) GATC sequences, DNA nicks and the MutH function in *Escherichia coli* mismatch repair. *EMBO J.*, **6**, 1121–1127.

Lu,A.-L., Clark,S. and Modrich,P. (1983) Methyl-directed repair of DNA base pair mismatches *in vitro*. *Proc. Natl Acad. Sci. USA*, **80**, 4639–4643.

Lu,A.-L., Welsh,K., Clark,S., Su,S.-S. and Modrich,P. (1984) Repair of DNA base-pair mismatches in extracts of *Escherichia coli*. *Cold Spring Harbor Symp. Quant. Biol.*, **49**, 589–596.

Makhov,A.M., Boehmer,P.E., Lehman,I.R. and Griffith,J.D. (1996) The herpes simplex virus type 1 origin-binding protein carries out origin specific DNA unwinding and forms unwound stem–loop structures. *EMBO J.*, **15**, 1742–1750.

Marquardt,D.W. (1963) An algorithm for least-squares estimation of non-linear parameters. *J. Soc. Ind. Appl. Math.*, **11**, 431–441.

Meselson,M. (1988) Methyl-directed repair of DNA mismatches. In Low,K.B. (ed.), *Methyl-Directed Repair of DNA Mismatches*. Academic Press, San Diego, pp. 91–113.

Modrich,P. (1991) Mechanisms and biological effects of mismatch repair. *Annu. Rev. Genet.*, **25**, 229–253.

Modrich,P. and Lahue,R. (1996) Mismatch repair in replication fidelity, genetic recombination, and cancer biology. *Annu. Rev. Biochem.*, **65**, 101–133.

Nevers,P. and Spatz,H. (1975) *Escherichia coli* mutants *uvrD uvrE* deficient in gene conversion of lambda heteroduplexes. *Mol. Gen. Genet.*, **139**, 233–243.

Pukkila,P.J., Peterson,J., Herman,G., Modrich,P. and Meselson,M. (1983) Effects of high levels of DNA adenine methylation on methyl-directed mismatch repair in *Escherichia coli*. *Genetics*, **104**, 571–582.

Radman,M. (1989) Mismatch repair and the fidelity of genetic recombination. *Genome*, **31**, 68–73.

Runyon,G.T., Wong,I. and Lohman,T.M. (1993) Overexpression, purification, DNA binding, and dimerization of the *E. coli uvrD* gene product (helicase II). *Biochemistry*, **32(2)**, 602–612.

Schleif,R. (1992) DNA looping. *Annu. Rev. Biochem.*, **61**, 199–223.

Su,S.-S. and Modrich,P. (1986) *Escherichia coli mutS*-encoded protein binds to mismatched DNA base pairs. *Proc. Natl Acad. Sci. USA*, **83**, 5057–5061.

Su,S.-S., Lahue,R.S., Au,K.G. and Modrich,P. (1988) Mispair specificity of methyl-directed DNA mismatch correction *in vitro*. *J. Biol. Chem.*, **263**, 6829–6835.

Wagner,R., Dohet,C., Jones,M., Doutriaux,M.-P., Hutchinson,F. and Radman,M. (1984) Involvement of *Escherichia coli* mismatch repair in DNA replication and recombination. *Cold Spring Harbor Symp. Quant. Biol.*, **49**, 611–615.

Welsh,K.M., Lu,A.-L., Clark,S. and Modrich,P. (1987) Isolation and characterization of the *Escherichia coli mutH* gene product. *J. Biol. Chem.*, **262**, 15624–15629.

Wu,T.H. and Marinus,M.G. (1994) Dominant negative mutator mutations in the *mutS* gene of *Escherichia coli*. *J. Bacteriol.*, **176**, 5393–5400.

Received on February 3, 1997; *revised on April 30, 1997*